

Reactivity of 1,4-Dihydropyridines Toward SIN-1-Derived Peroxynitrite

C. López-Alarcón,¹ H. Speisky,² J. A. Squella,¹
C. Olea-Azar,³ C. Camargo,⁴ and
Luis J. Núñez-Vergara^{1,5}

Purpose. To study the reactivity of C4-substituted 1,4-dihydropyridines (1,4-DHP), with either secondary or tertiary nitrogen in the dihydropyridine ring, toward SIN-1-derived peroxynitrite in aqueous media at pH 7.4.

Methods. Reactivity was followed by changes in the absorptivity of the UV-Vis bands corresponding to 1,4-DHP. Gas Chromatography/Mass Spectrometer (GC-MS) and Electron Paramagnetic Resonance (EPR) spin trap techniques were used to characterize the final product and the intermediates of the reaction, respectively.

Results. 1,4-DHPs significantly reacted toward peroxynitrite at varied rates, according to the calculated kinetic rate constants. By EPR spectroscopy, a carbon-centered radical from the 1,4-DHP was intercepted with *N-tert*-butylamine- α -phenylnitron (PBN), as the intermediate for the reaction with peroxynitrite. Likewise, the oxidized derivative (i.e., the pyridine) was identified as the final product of the reaction by GC-MS. By using the technique of deuterium kinetic isotope effect, the participation of the hydrogen of the 1-position on the 1,4-DHP ring was shown not to be the rate-limiting step of the reaction.

Conclusions. The direct participation of the 1,4-DHP derivatives in the quenching of SIN-1-derived peroxynitrite has been demonstrated. Kinetic rate constant of tested 1,4-DHP toward peroxynitrite showed a direct relationship with the oxidation peak potential values; that is, compounds reacting faster were more easily oxidized.

KEY WORDS: 1,4-dihydropyridines; EPR; GC-MS; kinetic rate constants; peroxynitrite.

INTRODUCTION

Peroxynitrite, ONOO⁻, is formed *in vivo* by the reaction of nitric oxide (NO[•]) with superoxide (1). The biological relevance of this species was first pointed out by Beckman *et al.* (2), who recognized that peroxynitrite may be formed in significant quantities under pathologic conditions. Because both NO[•] and O₂^{•-} are produced at high rates by phagocytic cells such as macrophages, relatively small increases in the rates of NO[•] and O₂^{•-} production may greatly increase the rate of

peroxynitrite formation, $v = k[\text{NO}^{\bullet}][\text{O}_2^{\bullet-}]$, reaching potentially cytotoxic levels.

Although the role of the peroxynitrite as a cytotoxic species *in vivo* is still debated (3), its associated form (i.e., the peroxynitrous acid) is a recognized oxidant and thereby it may destroy crucial cellular targets. On the other hand, the oxidizing capability of peroxynitrite toward a variety of biomolecules has widely been investigated and demonstrated *in vitro* (4).

The pathologic activity of peroxynitrite is presumably based on its capability to oxidize protein and nonprotein sulfhydryls (4), membrane phospholipids (5), low-density lipoproteins (6), and tyrosine residues (7). Under *in vivo* conditions, low amounts of peroxynitrite seem to be formed continuously (8). This process can be mimicked in experimental systems with the O₂^{•-} and NO[•] releasing compound SIN-1 (8). Peroxynitrite generated *in situ* from SIN-1 has been shown to attack many biological targets; for example, low-density lipoproteins in nearly the same manner as a bolus addition of authentic peroxynitrite (6).

The mechanisms of peroxynitrite reactions, such as conversion to nitrate, oxidation, and nitration, are controversial. Thus, the oxidation reactions mediated by peroxynitrite are expected to take place by complicated reaction pathways, and despite extensive research, no unified model is available as yet. Both one- and two-electron oxidation have been found in several reactions induced by peroxynitrite (9).

On the other hand, the 4-substituted Hantzsch 1,4-dihydropyridines (1,4-DHP), having at least a single hydrogen atom at the position 4, are interesting compounds not only from the point of view of the heterocyclic chemistry but also as pharmacologically active substances, due to their potential to act as antioxidants (10,11) and as NADH coenzyme analogs that mediate hydrogen transfer reactions in biological systems (12–14). More recently (15–17), the oxidation of Hantzsch 1,4-dihydropyridines has attracted much attention from chemists because of its reactivity toward endobiotics such as nitric oxide. The latter is coincident with the discovery of several active roles of NO[•] in a wide range of human pathological processes (18).

Furthermore, because peroxynitrite can react with reduced NADH (19), the study of the ability of 1,4-dihydropyridines to quench peroxynitrite seems also to be of interest. Taking into account the above, in the current work a systematic study on the reactivity of a number of 1,4-DHP with SIN-1-derived peroxynitrite was addressed. Kinetic rate constant values, reaction mechanisms, and a detailed discussion based on experimental results that relate the chemical structure and the oxidation potentials of the 1,4-DHP compounds are presented.

MATERIALS AND METHODS

Chemicals

All solvents were of high-pressure liquid chromatography (HPLC) grade and all reagents were of analytical grade.

Compounds

The following 1,4-dihydropyridine derivatives (Fig. 1, I–VI, VIII) were synthesized in our laboratory according to a previously described procedures (20,21). The final products

¹ Laboratory of Bioelectrochemistry, Faculty of Chemical and Pharmaceutical Sciences, University of Chile, Santiago, Chile.

² Nutritional Toxicology, INTA, Faculty of Chemical and Pharmaceutical Sciences, University of Chile, Santiago, Chile.

³ Department of Inorganic and Analytical Chemistry, Faculty of Chemical and Pharmaceutical Sciences, University of Chile, Santiago, Chile.

⁴ Laboratory of Antidoping, Faculty of Chemical and Pharmaceutical Sciences, University of Chile, Santiago, Chile.

⁵ To whom correspondence should be addressed. (e-mail: lnunezv@ciq.uchile.cl)

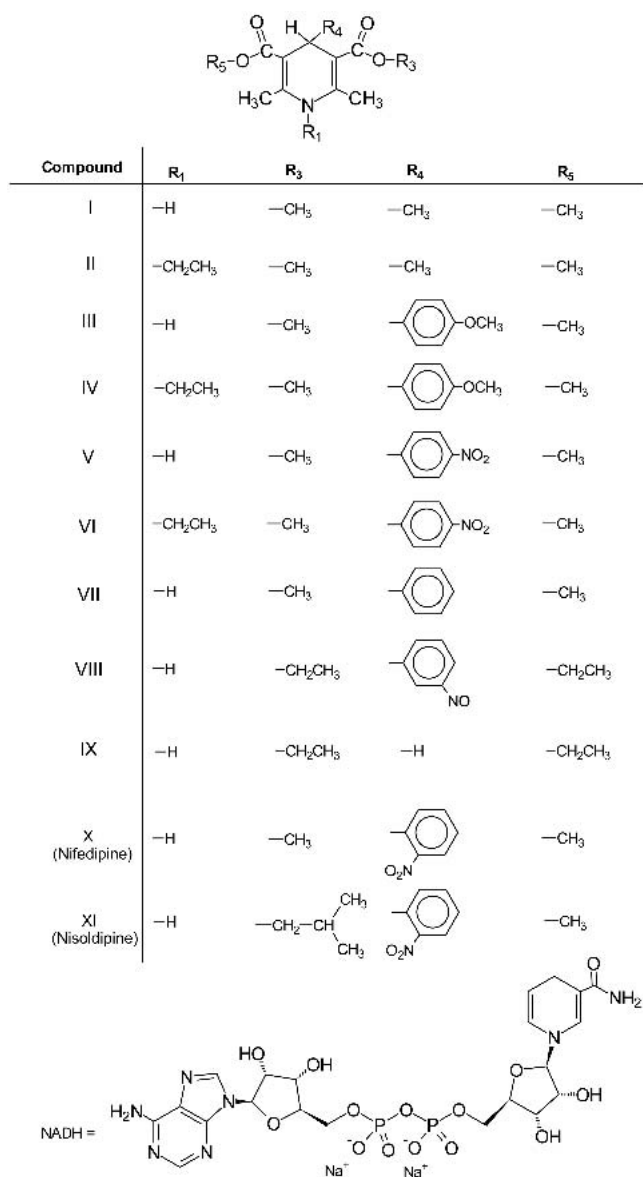


Fig. 1. Chemical structures of 1,4-dihydropyridines and NADH.

were subjected to IR, NMR, and elemental analyses obtaining the following results:

I. 4-Methyl-2,6-dimethyl-3,5-dimethoxycarbonyl-1,4-dihydropyridine.

IR (KBr): ν_{\max} 3342, 2950, 1680, 1650, 1435, 1351, 1226, 1056, cm^{-1} .

^1H NMR (300 MHz, CDCl_3): δ 0.96 (d, 3H, $J = 6.5\text{Hz}$, $>\text{CH}-\text{CH}_3$), 2.29 (s, 6H, $-\text{CH}_3$), 3.73 (s, 6H, $-\text{O}-\text{CH}_3$), 3.83 (q, 1H, $J = 6.5\text{Hz}$, $>\text{CH}-\text{CH}_3$), 5.73 (s, 1H, $-\text{NH}-$). ^{13}C NMR (75 MHz, CDCl_3): (20.35x2), 23.20, 29.30, (51.92x2), (105.27x2), (145.64x2), (169.19x2). Anal. Calcd. for $\text{C}_{12}\text{H}_{17}\text{O}_4\text{N}$: C, 60.25; H, 7.13; N, 5.86. Found: C, 60.27; H, 7.23; N, 5.87. m.p.: 147°C – 149°C .

II. 4-Methyl-2,6-dimethyl-3,5-dimethoxycarbonyl-N-ethyl-1,4-dihydropyridine.

IR (KBr): ν_{\max} 2954, 1696, 1631, 1434, 1389, 1212, 1163, 1056 cm^{-1} .

^1H NMR (300 MHz, CDCl_3): δ 0.88 (d, 3H, $J = 6.6\text{Hz}$, $>\text{CHCH}_3$), 1.16 (t, 3H, $J = 7.1\text{Hz}$ N- CH_2CH_3), 2.4 (s, 6H, $-\text{CH}_3$), 3.7 (q, 2H, $J = 7.1\text{Hz}$ N- CH_2CH_3), 3.72 (s, 6H, $-\text{OCH}_3$), 3.77 (q, 1H, $J = 6.6\text{Hz}$, $>\text{CHCH}_3$). ^{13}C NMR (75 MHz, CDCl_3): 15.56, (16.15x2), 21.73, 28.12, 39.51, (51.12x2), (108.75x2), (148.01x2), (168.50x2). Anal. Calcd. for $\text{C}_{14}\text{H}_{21}\text{NO}_4$: C, 62.84; H, 7.85; N, 5.23. Found: C, 63.05; H, 7.62; N, 5.13. m.p.: 78°C – 80°C .

III. 4-(4-methoxyphenyl)-2,6-dimethyl-3,5-dimethoxycarbonyl-1,4-dihydropyridine.

IR (KBr): ν_{\max} 3349, 2949, 1697, 1650, 1431, 1383, 1251, 1213, 1027 cm^{-1} .

^1H NMR (300 MHz, CDCl_3): δ 2.33 (s, 6H, $-\text{CH}_3$), 3.65 (s, 6H, $-\text{O}-\text{CH}_3$), 3.75 (s, 3H, Ar- $\text{O}-\text{CH}_3$), 4.94 (s, 1H, Ar- $\text{CH}<$), 5.76 (s, 1H, $-\text{NH}-$), 6.75 (d, 2H, $J = 8.6\text{Hz}$, Ar-H), 7.2 (d, 2H, $J = 8.6\text{Hz}$, Ar-H). ^{13}C NMR (75 MHz, CDCl_3): (19.51x2), 38.31, (50.94x2), 55.05, (104.00x2), (113.30x2), (128.53x2), 139.86, (143.93x2), 157.85, (168.06x2). Anal. Calcd. for $\text{C}_{18}\text{H}_{21}\text{O}_5\text{N}$: C, 65.24; H, 6.39; N, 4.23. Found: C, 65.00; H, 6.47; N, 4.36. m.p.: 181°C – 183°C .

IV. 4-(4-Methoxyphenyl)-2,6-dimethyl-3,5-dimethoxycarbonyl-N-ethyl-1,4-dihydropyridine.

IR (KBr): ν_{\max} 2948, 1690, 1629, 1433, 1390, 1256, 1213, 1152, 1035 cm^{-1} .

^1H NMR (300 MHz, CDCl_3): δ 1.06 (t, 3H, $J = 5.9\text{Hz}$ N CH_2-CH_3), 2.47 (s, 6H, $-\text{CH}_3$), 3.67 (q, 2H, $J = 5.9\text{Hz}$ N- CH_2CH_3), 3.7 (s, 6H, $-\text{OCH}_3$), 3.75 (s, 3H, Ar- OCH_3), 5.04 (s, 1H, Ar- $\text{CH}<$), 6.75 (d, 2H, $J = 8.7\text{Hz}$, Ar-H), 7.09 (d, 2H, $J = 8.7\text{Hz}$, Ar-H). ^{13}C NMR (75 MHz, CDCl_3): 16.06, (16.42x2), 37.19, 40.42, (51.26x2), 55.17, (107.16x2), (113.32x2), (127.91x2), 138.53, (148.53x2), 157.90, (168.61x2). Anal. Calcd. for $\text{C}_{20}\text{H}_{25}\text{NO}_5$: C, 66.77; H, 6.96; N, 3.9. Found: C, 66.85; H, 7.08; N, 3.66. m.p.: 106°C – 108°C .

V. 4-(4-Nitrophenyl)-2,6-dimethyl-3,5-dimethoxycarbonyl-1,4-dihydropyridine.

IR (KBr): ν_{\max} 3343, 2948, 1703, 1655, 1518, 1434, 1384, 1347, 1218, 1020 cm^{-1} .

^1H NMR (300 MHz, CDCl_3): δ 2.38 (s, 6H, $-\text{CH}_3$), 3.66 (s, 6H, $-\text{O}-\text{CH}_3$), 5.12 (s, 1H, Ar- $\text{CH}<$), 5.85 (s, 1H, $-\text{NH}-$), 7.46 (d, 2H, $J = 8.8\text{Hz}$, Ar-H), 8.12 (d, 2H, $J = 8.8\text{Hz}$, Ar-H). ^{13}C NMR (75 MHz, CDCl_3): (20.63x2), 40.73, (52.11x2), (103.92x2), (124.39x2), (129.53x2), (145.81x2), 147.29, 155.64, (168.38x2). Anal. Calcd. for $\text{C}_{17}\text{H}_{18}\text{O}_6\text{N}_2$: C, 58.96; H, 5.24; N, 8.09. Found: C, 58.76; H, 5.03; N, 8.25. m.p.: 165°C – 168°C .

VI. 4-(4-Nitrophenyl)-2,6-dimethyl-3,5-dimethoxycarbonyl-N-ethyl-1,4-dihydropyridine.

IR (KBr): ν_{\max} 2945, 1690, 1624, 1511, 1382, 1345, 1252, 1154, 1025 cm^{-1} .

^1H NMR (300 MHz, CDCl_3): δ 1.04 (t, 3H, $J = 7.1\text{Hz}$, N- CH_2CH_3), 2.5 (s, 6H, $-\text{CH}_3$), 3.72 (s, 6H, $-\text{OCH}_3$), 3.72 (q, 2H, $J = 7.1\text{Hz}$, N- CH_2-CH_3), 5.19 (s, 1H, Ar- $\text{CH}<$), 7.34 (d, 2H, $J = 8.5\text{Hz}$, Ar-H) 8.07 (d, 2H, $J = 8.5\text{Hz}$, Ar-H). ^{13}C NMR (75 MHz, CDCl_3): 16.06, (16.4x2), 38.25, 40.0, (51.44x2), (105.70x2), (123.29x2), (127.74x2), (146.42x2), 149.32, 153.61, (167.94x2). Anal. Calcd. for $\text{C}_{19}\text{H}_{22}\text{N}_2\text{O}_6$: C, 60.9; H, 5.88; N, 7.48. Found: C, 61.10; H, 5.99; N, 7.34. m.p.: 156°C – 157°C .

VIII. 4-(3-Nitrosophenyl)-2,6-dimethyl-3,5-diethoxy-carbonyl-1,4-dihydropyridine.

IR (KBr): ν_{\max} 3334.5, 29981.7, 1699.8, 1651.3, 1488.8, 1371, 1300.2, 1213.3, 1102.1, 1020.2 cm^{-1} .

$^1\text{H-NMR}$ (300MHz, CDCl_3): δ 1.2(t, 6H, $J = 7.2$ Hz, $-\text{CH}_2\text{CH}_3$), 2.36(s, 6H, R- CH_3), 4.1(m, 4H, $-\text{CH}_2\text{CH}_3$), 5.1(s, 1H, $>\text{CH}-$), 5.7(s, 1H, $>\text{NH}$), 7.7(m, 4H, Ar-H) ppm. ^{13}C NMR (75 MHz, CDCl_3): (2x13.2302); (2x18.5819); 38.852; 58.9277, 102.533; 118.131; 119.819; 127.550; 128.035; 134.542; 143.681; (2x148.692); 165.457; 165.796; 166.248; 167.671 ppm. Calc. $\text{C}_{19}\text{H}_{22}\text{O}_5\text{N}_2$: C = 63.67; H, 6.29; N, 7.62. Found: C, 63.52; H, 6.36; N, 7.66. mp: 118.2°C–119.1°C.

NMR spectroscopy: The NMR spectra were recorded on a Bruker spectrometer Avance DRX 300 (Rheinstetten, Karlsruhe, Germany).

FT-IR: The IR spectra were recorded on a Bruker spectrometer IFS 55 Equinox (Rheinstetten, Karlsruhe, Germany).

Elemental analyses were performed in a Fisons Instrument equipment (Fisons-Carlo Erba modelo EA 1108 (Milano, Italy)).

Drugs

Nisoldipine and nifedipine were supplied by Sanitas Laboratories (Santiago, Chile). Both compounds were assayed without previous purification. NADH was obtained from Merck.

Solutions

Care was taken to exclude possible contamination by bicarbonate/carbon dioxide. Milli-Q water ($\Omega = 18.6$) was bubbled with oxygen for 30 min. Potassium phosphate buffer (KH_2PO_4 , 50 mM)/acetonitrile, 70/30 (v/v) solutions were prepared on the day of the experiments and pH adjusted to 7.4 at 37°C.

Experimental Conditions

SIN-1 (Aldrich Chemical Co.) was used as peroxyxynitrite generator (Fig. 2). SIN-1 (100 μM) was added to 3 ml of 1,4-DHP or NADH (50 μM) solutions in potassium phosphate buffer/acetonitrile 70/30 (v/v) at pH 7.4. The final solutions were incubated between 1 and 2.5 h at 37°C. The progress of the reaction was followed both via UV and Vis spectroscopy. The final products were analyzed by gas chromatograph/mass spectrometer (GC-MS).

UV-Vis

The progress of the reaction with SIN-1-derived peroxyxynitrite was followed by UV-Vis spectroscopy using an

UNICAM UV-3 spectrophotometer (Cambridge, UK). Acquisition and data treatment were carried out with a 2.11 software (Vision software, Unicam Limited, Cambridge, UK). UV-Vis spectra were recorded in the 220–500 nm range at different intervals. For all compounds the absorption bands at 330–370 nm were used. Drug concentrations in aqueous buffer [KH_2PO_4 50 mM/acetonitrile, 70/30 (v/v) pH 7.4] were determined from respective calibration curves (10–100 μM). The rates of the reactions were calculated using the kinetic rate constant between NADH and SIN-1-derived peroxyxynitrite reported in the literature, $k = 1 \times 10^4 \text{ m}^{-1} \text{ s}^{-1}$ (19).

Control solutions (in the absence of SIN-1) revealed no changes either in their original UV-Vis absorption bands or GC-MS mass fragmentation.

Also, a possible photodecomposition of 1,4-dihydropyridines was assessed, but in the time-scale of the experiments this was negligible.

GC-MS

A Gas Chromatograph/Mass Spectrometer Hewlett Packard 5890/5972 Detector (Palo Alto, CA, USA) and Hewlett Packard 7673 Autosampler were used for the measurements. A Hewlett Packard Pentium II Data System-Laser Jet 4000 printer, controlled instrumentation, and data handling was also used.

Chromatography Column

Hewlett-Packard Ultra-1 column, 25 m \times 0.2 mm i.d. \times 0.11 film thickness (Little Falls, Wilmington, Delaware, USA).

Chromatographic Conditions

Detector temperature, 300°C; injector temperature, 250°C; split ratio, 1/10; pressure, 13 psi; purge flow, 40 ml min^{-1} ; purge time, 0.5 ml min^{-1} .

Temperature Program

The oven temperature was programmed from 130°C to 305°C (hold for 5 min) at 15°C min^{-1} ; run time was 16.67 min. Helium was used as carrier gas with an inlet pressure of 35 kPa. The identification of the samples was based on the analyses of the mass spectra (full scan).

After the reaction, the final solutions were diluted and injected without any pretreatment. Consequently, no extraction or filtration procedures were necessary.

Deuterium Kinetic Isotope Effect (DKIE) Studies

Studies by $^1\text{H-NMR}$ Spectroscopy

In order to establish the exchange among the proton of the position 1 with a deuterium atom, compound I was dis-

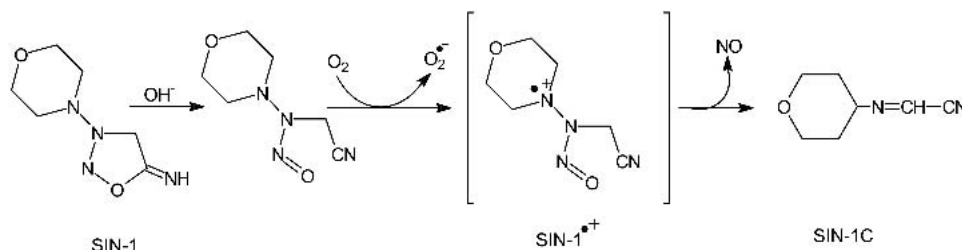


Fig. 2. Reaction scheme of peroxyxynitrite formation from SIN-1.

solved in DMSO- d_6 carrying out a normal $^1\text{H-NMR}$. After this, 20 μl D_2O was added to the sample in order to observe the possible change in the typical $-\text{NH}-$ signal.

DKIE Influence on the Kinetic Rate Constants of Compound I

Both, control solutions [$\text{H}_2\text{O}/\text{DMSO}$ 70/30 (v/v) in 50 mM phosphate buffer pH 7.4] and deuterated solutions [$\text{D}_2\text{O}/\text{DMSO-}d_6$ 70/30 (v/v) in 50 mM phosphate buffer pH 7.4] containing 50 μM of compound I were incubated at 37°C for 2 h. Then, the same experimental procedure as was previously described was followed (Experimental conditions and UV-Vis sections).

Electron Paramagnetic Resonance Studies

The EPR spectra were recorded *in situ* on a Bruker spectrometer ECS 106 (Rheinstetten, Karlsruhe, Germany) with 100 kHz field modulation in X band (9.78 GHz) at room temperature. The hyperfine splitting constants were estimated to be accurate within 0.05 G.

Two types of studies were performed: a) controlled potential electrolysis of 1 mM Compound I solutions in 50 mM phosphate/acetonitrile (70/30, v/v) at pH 7.4. These studies were performed in the EPR cell using an appropriate platinum mesh electrode at 1.0 V vs. Ag/AgCl in the presence of 100 mM spin trap, *N-tert*-butylamine- α -phenylnitron (PBN). The spin trap was electrochemically tested for purity, as was the magnitude of the so-called potential window (the potential range within which the trap is electrochemically inactive). The oxidation peak potential of PBN in 50 mM phosphate/acetonitrile (70/30) at a Pt electrode was + 1.42 V vs. Ag/AgCl. EPR spectra were collected after 20 min of electrolysis. b) Reaction of 1 mM Compound I solutions in the presence of 100 mM PBN and 2 mM SIN-1 in 50 mM phosphate/acetonitrile (70/30, v/v) at pH 7.4 were analyzed by EPR. Spectra were collected up to 1 h of reaction.

Also, two types of blank solutions containing 2 mM SIN-1 + 100 mM PBN and 1 mM compound I + 100 mM PBN were analyzed by EPR in the same experimental conditions. Under the experimental conditions, none of these solutions revealed any signal.

Voltammetry

Differential pulse voltammetry (DPV) was performed with a BAS CV50, (Bioanalytical Systems, West Lafayette, USA) assembly. A glassy carbon stationary electrode was used as working electrode. A platinum wire was used as a counterelectrode, and all potentials were measured against an Ag/AgCl electrode.

Operating conditions: pulse amplitude, 40 mV; potential scan, 4 mVs^{-1} ; voltage range, 0 to 1000 mV, current range, 5 to 25 μA , temperature, 25°C. All the solutions were purged with pure nitrogen for 10 min before the voltammetric runs.

RESULTS AND DISCUSSION

Reactivity of 1,4-DHP Toward SIN-1-Derived Peroxynitrite: UV-Vis Spectroscopic Studies

The 1,4-DHP tested compounds displayed UV absorption bands that ranged typically between $\lambda = 330$ and 430 nm and were maximal between 330 nm and 370 nm (Fig. 3). A sustained decrease of the maximal UV bands was observed

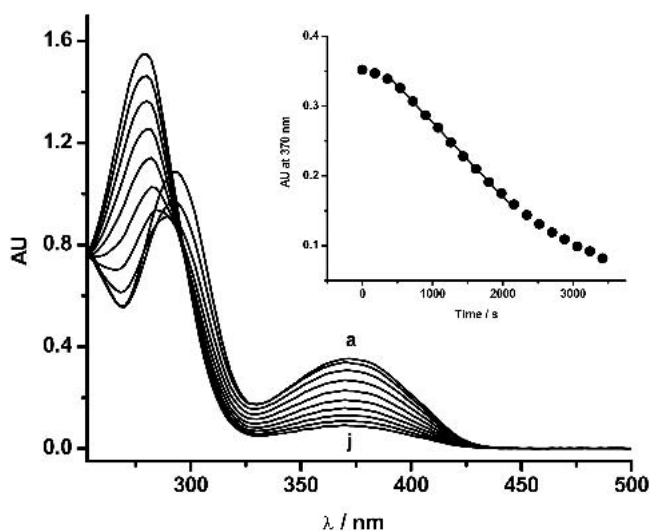


Fig. 3. Time-course of UV-Vis spectra corresponding to the reaction between 50 μM compound IX and 100 μM SIN-1-derived peroxy-nitrite in 50 mM phosphate buffer/acetonitrile (70/30) at pH 7.4. a-j: 60 min. Inset: Time-course of the UV absorption at 370 nm.

following the addition of 100 μM SIN-1 to an aqueous solution (pH 7.4) containing the 1,4-DHP compounds. This effect is illustrated in Fig. 3 for compound IX. To compare the reactivity, kinetic rate constant values (k) were calculated as described in “Materials and Methods” for the tested 1,4-DHP derivatives (Table I). Also, we checked the rate of reaction of NADH with peroxy-nitrite following the decrease in absorbance at 340 nm. However, for comparative purposes, a reported k value for NADH of $1 \times 10^4 \text{ m}^{-1}\text{s}^{-1}$ was used (19).

Table I shows that all the 1,4-DHP derivatives reacted with peroxy-nitrite at varied rates; the C-4 unsubstituted 1,4-

Table I. Kinetic Rate Constants (k) for the Reaction Between SIN-1-Derived Peroxynitrite and 1,4-DHP and their Relationship with NADH and the Oxidation Peak Potentials

Compound	$k \times 10^{-3}/\text{M}^{-1} \text{ s}^{-1a}$	$k_{1,4\text{-DHP}}/k_{\text{NADH}}^b$	Ep/mV^c
I	3.0 ± 0.1	0.3	660
II	1.0 ± 0.05	0.1	748
III	3.0 ± 0.2	0.3	680
IV	0.8 ± 0.06	0.08	772
V	1.8 ± 0.12	0.18	768
VI	0.5 ± 0.03	0.05	830
VII	2.5 ± 0.12	0.25	660
VIII	1.8 ± 0.08	0.18	742
IX	10.3 ± 0.4	1.03	352
X (nifedipine)	1.1 ± 0.07	0.11	744
XI (nisoldipine)	1.0 ± 0.08	0.1	681
NADH	10	1.0	492

^a Kinetic rate constants were calculated by using the kinetic rate constant for the reaction between NADH and SIN-1-derived peroxy-nitrite ($k = 1 \times 10^4 \text{ M}^{-1} \text{ s}^{-1}$, taken from Ref. 19).

^b Ratio between kinetic rate constants of the tested 1,4-DHP derivatives/kinetic rate constant of NADH in presence of SIN-1.

^c Oxidation peak potential values determined by differential pulse voltammetry using a glassy carbon working electrode in 50 mM phosphate buffer/acetonitrile (70/30, v/v) + 0.1 M KCl at pH 7.4. Potentials are expressed vs. Ag/AgCl reference electrode. 1,4-DHP concentration: 0.1 mM

DHP (compound IX) being the most reactive one, exhibiting a k value of $1.03 \times 10^4 \text{ m}^{-1}\text{s}^{-1}$, which was similar to that described for NADH (19). Such a result could be explained by the similarity of the chemical moiety involved in the reaction; that is, 1,4-dihydropyridine ring vs. N-substituted nicotinamide (Fig. 1).

Compound IX shows a range of reactivity between 20.6 and 3.4 times higher than that of the other tested C-4 substituted 1,4-DHP derivatives (Table I). Also, compound IX was found to be more reactive than the two well-known 1,4-DHP, nifedipine and nisoldipine.

The inclusion of an electron-donor group on the C-4 phenyl moiety slightly increased (by 20%) the rate of reaction (compound III vs. compound VII). In contrast, the inclusion of an electron-withdrawing group on the C-4 phenyl moiety gave rise to a slight decrease (of 28%) in the k value (compound V vs. compound VII).

On the other hand, the N-alkylation of the 1-position produced a significant decrease of the reaction rates (Table I). Comparing compound V and compound VIII, no differences in their k values were found; the latter despite the well-known spin-trapping properties of the nitroso group (22).

Reaction Mechanism

In order to investigate the possible reaction mechanism, different techniques were used for this purpose. These included GC-MS technique to identify final product (s), deuterium kinetic isotope effect (DKIE) studies to determine the participation of the hydrogen of the 1-position in rate of reaction, and EPR studies to assess the possible formation of radical species as intermediates from the 1,4-DHP after the reaction with SIN-1-derived peroxyntirite. Also, correlations between oxidation potentials and kinetic rate constants are reported.

GC-MS Technique

In the following section, the identification of the products obtained after the reaction between the 1,4-DHP derivatives and peroxyntirite is shown. The chromatographic data corresponding to the 1,4-DHP compounds and their corresponding oxidized derivatives are shown in Tables II and III. Some conclusions on these studies can be summarized as follows: a) The GC-MS procedure used to characterize the par-

Table II. GC-MS Characteristics of Parent 1,4-DHP

Compound	1,4-DHP		Rt/min.
	Bp	M ⁺	
I	224	239	6.2
II	252	267	6.9
III	224	331	10.5
IV	300	359	11.0
V	224	346	11.9
VI	315	374	12.3
VII	224	301	9.2
VIII	252	358	11.3
IX	224	253	7.1
X	329	346	10.3
XI	371	388	11.4

Bp: Base peak; M⁺: Mass-charge ion; Rt/min: Retention time in minutes.

Table III. GC-MS Characteristics of the Oxidized Derivatives Obtained After the Reaction Between 1,4-DHP with SIN-1-Derived Peroxyntirite

Compound	Oxidized derivatives		
	Bp	M ⁺	Rt/min.
I. Pyridine	206	237	4.8
II. Pyridinium salt	—	—	—
III. Pyridine	266	329	8.7
IV. Pyridinium salt	—	—	—
V. Pyridine	313	344	9.6
VI. Pyridinium salt	—	—	—
VII. Pyridine	236	299	7.3
VIII. Pyridine	342	356	9.9
IX. Pyridine	206	251	5.7
X. Pyridine	298	344	9.1
XI. Pyridine	284	386	10.2

Bp: Base peak; M⁺: Mass-charge ion; Rt/min: Retention time in minutes.

ent 1,4-DHP and its subsequent reactivity with peroxyntirite did not require derivatization. b) After the reaction with peroxyntirite, the 1,4-DHP suffered a dehydrogenation process yielding the pyridine-derivative. The latter conclusion is supported by the respective retention times and mass fragmentation pattern for each compound as displayed in Table III. Noteworthy, in the scavenging of peroxyntirite by 1,4-DHP, an electron transfer reaction is involved. c) Retention times of the corresponding pyridine derivatives were lower than that of the parent compounds (Fig. 4). d) The mass fragmentation pattern of the aromatized derivatives shows different peak bases, depending on C-4 substitution on the 1,4-dihydropyridine ring. e) The reaction between N-ethyl-DHP derivatives with peroxyntirite, as assessed by the GC-MS technique, did not reveal any new signal. Thus, the lack of a new signal observed by this technique could be explained on the basis of our previous observation that the electrochemical oxidation of N-substituted DHP gives rise to a pyridinium salt as a final product (23). This final product is soluble in aqueous media preventing its subsequent extraction to inject it into a chromatograph (24).

Deuterium Kinetic Isotope Effect Studies

To assess the feasibility of participation of the hydrogen in the 1-position, DKIE studies were carried out selecting compound I. As noted from the NMR experiments, the addition of 20 μl D₂O to a solution of compound I (600 μl) made the -NH- signal at 8.7 ppm disappear, thus demonstrating that the proton of the secondary amine group was isotopically exchanged with deuterium. A detailed experimental description of the ¹H-NMR signals is as follows:

a. Normal spectra corresponding to compound I:

¹H-NMR (300 MHz, DMSO-*d*₆): δ 0.82 (d, 3H, J = 6.4 Hz, >CH-CH₃), 2.2 (s, 6H, -CH₃), 3.6 (s, 6H, -O-CH₃), 3.7 (q, 1H, J = 6.4 Hz, >CH-CH₃), 8.7 (s, 1H, -NH-).

b. Spectra of compound I with addition of deuterium oxide:

¹H-NMR (300 MHz, DMSO-*d*₆+D₂O): δ 0.82 (d, 3H, J = 6.4 Hz, >CH-CH₃), 2.2 (s, 6H, -CH₃), 3.6 (s, 6H, -O-CH₃), 3.7 (q, 1H, J = 6.4 Hz, >CH-CH₃).

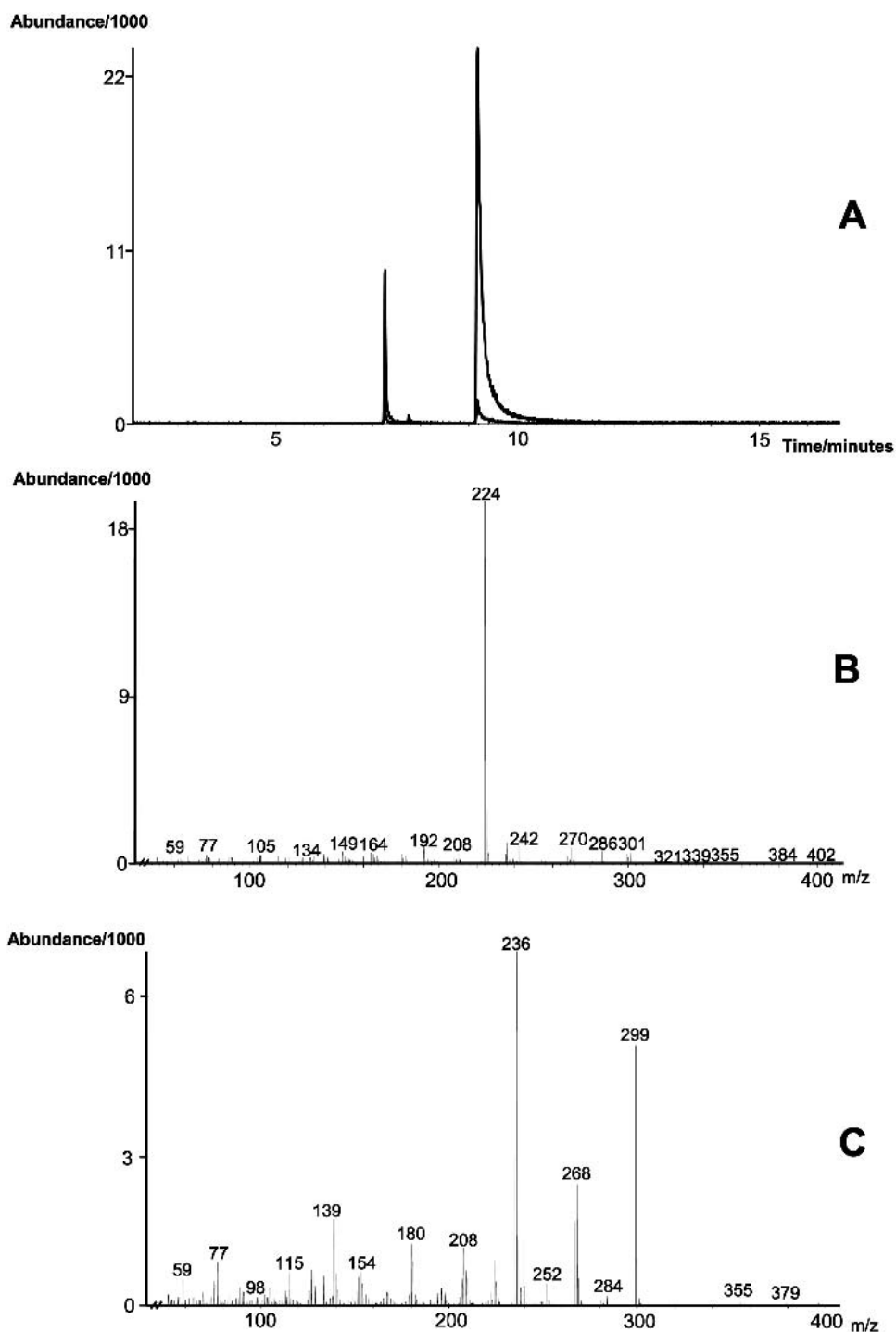


Fig. 4. Ion chromatogram (A) and mass spectrum corresponding to compound VII after the reaction with peroxyntirite (B) and its corresponding pyridine derivative (C).

The kinetic constant corresponding to the deuterated compound I was estimated as described in "Materials and Methods." The ratio k_H/k_D for the peroxyntirite/compound I reaction was 1.3. Because this value falls below 2 (25), our experimental value of 1.3 can be interpreted as an indication that the hydrogen abstraction would not be the rate-limiting step of the reaction (25). However further studies should be conducted to clarify this, mainly to explore the possibility that a more complex mechanism of reaction with this oxidizing agent (peroxyntirite) is taking place.

EPR Spin-Trapping Studies

In order to gather evidence on the possible formation of a radical as an intermediate during the oxidation of 1,4-DHP induced by peroxyntirite, EPR experiments using the spin trap *N-tert*-butylamine- α -phenylnitrone (PBN) were carried out.

For comparative purposes, the trapping of the radical intermediates generated in the electrochemical oxidation of 1,4-DHP by PBN were also followed.

Figure 5 displays the EPR spectra correspond to the radicals intercepted with PBN during a controlled potential electrolysis (CPE) of compound I (part 5 A), and during the reaction between compound I and SIN-1-derived peroxy-nitrite (part 5 B). The spectrum C corresponds to the base line (see "Materials and Methods"). Spectra characteristics corresponding to a nitroxide spin adduct appeared in both, the electrodic reaction and the reaction with peroxy-nitrite in the presence of PBN. The EPR spectra show the triplet, due to the nitrogen, and its splitting into a doublet due to the presence of the adjacent hydrogen. a_N values around 14 G and a_H splitting values of 3 G were obtained for the 1,4-DHP spin adduct. The splitting constants for the spin adduct of about 14 G are consistent with the fact that PBN interacted with carbon-centered radicals as reported for 1,4-DHP derivatives (26) and for other structurally related compounds (27).

Previous work conducted by us (28) and others (29) shows that the electro-oxidation of 1,4-DHP derivatives yields different types of radical intermediates: primarily the radical cation $\text{PyH}^{\bullet+}$, and after its deprotonation, the neutral radical $\text{Py}\cdot$. According to the current EPR spectra results, it seems likely that the species added to the PBN spin trap is a pyridinium radical. From previous quantum chemical calculations (30), it follows that the unsubstituted pyridinium radical, $\text{Py}\cdot$, has the unpaired electron possibly localized in the 2-, 4-, or 6- position; however, the 4-position seems to be the preferred one (30). In addition, electronegative substituents in 3- and 5-position increase the spin density in the vicinal positions. Such effects are additive in 4-position, leading to an even greater preference for this position. Consequently, one

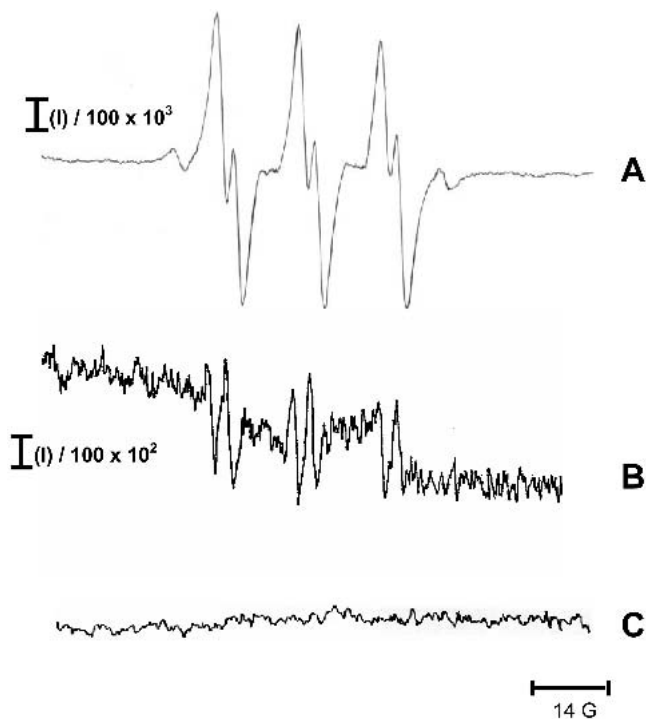


Fig. 5. Experimental EPR spectra of adduct PBN-pyridinium radical. (A) Radical electrochemically generated from 1 mM compound I solution in 50 mM phosphate buffer/acetonitrile (70/30). (B) Radical generated after the reaction between 1 mM compound I and 2 mM SIN-1. (C) Base line [2 mM SIN-1 + 100 mM PBN in 50 mM phosphate buffer/acetonitrile (70/30) at pH 7.4].

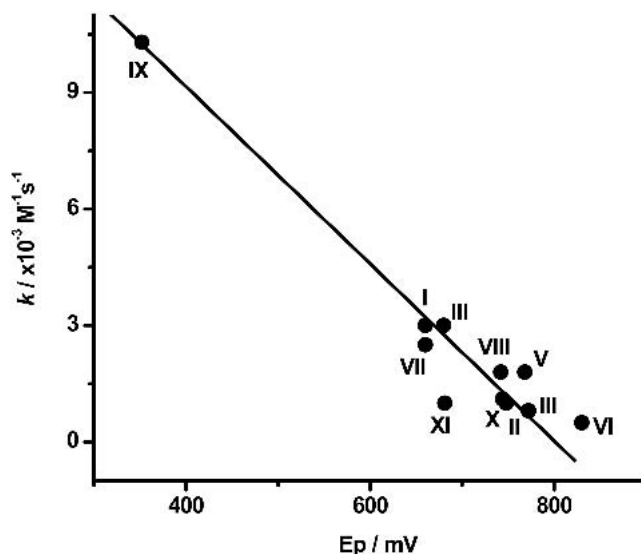


Fig. 6. Relationship between kinetic rate constants (k) for the reaction with peroxy-nitrite and the oxidation peak potentials of the 1,4-DHP derivatives at pH 7.4.

may assume that the radicals generated in our experiments are preferentially added to the spin trap by this C-4 reactive position.

Correlations Between Kinetic Rate Constants and Oxidation Peak Potential Values

Because it is demonstrated that the metabolism of 1,4-DHP used in the treatment of hypertension proceeds through oxidation (i.e., aromatization) of 1,4-DHP, significant research has been carried out to study the features of these oxidations (31). Therefore, in this section, attempts to correlate oxidation peak potential values, determined in aqueous media at pH 7.4, with kinetic rate constants for the reaction with SIN-1-derived peroxy-nitrite are discussed.

The electrochemical oxidation of the 1,4-dihydropyridines was studied in the same experimental conditions used in the reactivity studies (aqueous media). Under these conditions, all compounds exhibited only a single oxidation peak, which is consistent with previous reports (28,29). Figure 6 displays the relationship between the kinetic rate constants and the oxidation peak potentials. Data obtained

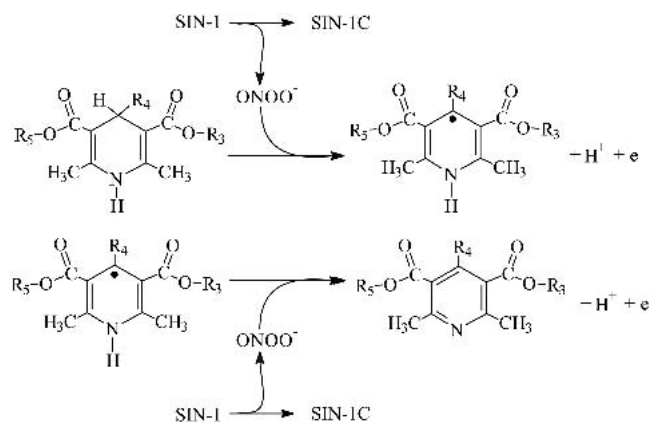


Fig. 7. Scheme for the reaction between 1,4-DHP and SIN-1-derived peroxy-nitrite.

from these studies indicate that the kinetic rate constants for the reaction between 1,4-DHP compounds and SIN-1-derived peroxyxynitrite exhibited a fairly good linear correlation with oxidation peak potential (kinetic rate constant = 17,000 – 21.04 Ep mV; c.c. = 0.96018). Thus, it is concluded that the compounds that are more easily oxidized are those that react more rapidly with peroxyxynitrite (Fig. 6).

CONCLUSIONS

1. In the current paper, we have demonstrated the direct participation of the 1,4-DHP derivatives in the quenching of SIN-1-derived peroxyxynitrite.

2. N-alkylation of the 1-position produced a significant decrease of the kinetic reaction rate.

3. In the electrode reaction and in the reaction with peroxyxynitrite carried out in the presence of PBN, spectra characteristics to a nitroxide spin adduct appeared. The splitting constants for the spin adduct are consistent with the fact that PBN interacted with carbon-centered radicals as previously reported for 1,4-DHP derivatives.

4. DKIE studies clearly demonstrate that the hydrogen abstraction would not be the rate-limiting step of the reaction.

5. After the reaction between 1,4-DHP and peroxyxynitrite, the pyridine derivative was formed as the final product.

6. Kinetic rate constant of tested 1,4-DHP toward peroxyxynitrite showed a direct relationship with the oxidation peak potential values (i.e., compounds reacting faster were more easily oxidized).

7. Based on the experimental evidences obtained in the current paper, a general mechanism as appears in Fig. 7 can be proposed.

ACKNOWLEDGMENTS

This work was partially supported by grants from FONDECYT 8000016. Also, the support of DID of University of Chile is acknowledged.

REFERENCES

1. B. Alvarez, H. Rubbo, M. Kirk, S. Barnes, B. A. Freeman, and R. Radi. Peroxyxynitrite-dependent tryptophan nitration. *Chem. Res. Toxicol.* **9**:390–396 (1996).
2. J. S. Beckman, T. W. Beckman, J. Chen, P. A. Marshall, and B. A. Freeman. Apparent hydroxyl radical production by peroxyxynitrite: implications for endothelial injury from nitric oxide and superoxide. *Proc. Natl. Acad. Sci. U S A* **87**:1620–1624 (1990).
3. J. M. Fukoto and L. J. Ignarro. In vivo aspects of nitric oxide (NO) chemistry: Does peroxyxynitrite (–OONO) play a major role in cytotoxicity. *Acc. Chem. Res.* **30**:149–152 (1997).
4. R. Radi, J. S. Beckman, K. M. Bush, and B. A. Freeman. Peroxyxynitrite oxidation of sulphydryls. *J. Biol. Chem.* **266**:4244–4250 (1991).
5. R. Radi, J. S. Beckman, K. M. Bush, and B. A. Freeman. Peroxyxynitrite-induced membrane lipid peroxidation: the cytotoxic potential of superoxide and nitric oxide. *Arch. Biochem. Biophys.* **288**:481–487 (1991).
6. C. R. White, T. A. Brock, L. Y. Chang, J. Crapo, P. Briscoe, D. Ku, W. A. Bradley, S. H. Gianturco, J. Gore, B. A. Freeman, and M. M. Tarpey. Superoxide and peroxyxynitrite in atherosclerosis. *Proc. Natl. Acad. Sci. U S A* **91**:1044–1048 (1994).
7. N. W. Kooy, J. A. Royall, Y. Z. Ye, D. R. Kelly, and J. S. Beckman. Evidence for in vivo peroxyxynitrite production in human acute lung injury. *Am. J. Respir. Crit. Care Med.* **151**:1250–1254 (1995).
8. R. E. Huie and S. Padmaja. The reaction of NO with superoxide. *Free Rad. Res. Comm.* **18**:195–199 (1993).
9. K. N. Houk, K. R. Condroski, and W. A. Pryor. Radical and

concerted mechanisms in oxidations of amines, sulfides and alkenes by peroxyxynitrite, pernitrous acid and the peroxyxynitrite CO₂ adduct: density functional theory transitions structures and energetics. *J. Am. Chem. Soc.* **118**:13002–13006 (1996).

10. G. Sobal, E. J. Menzel, and H. Sinzinger. Calcium antagonists in inhibitors of *in vitro* low density lipoprotein oxidation and glycation. *Biochem. Pharmacol.* **61**:373–379 (2001).
11. C. Napoli, M. Chiariello, G. Palumbo, and G. Ambrosio. Calcium channel blockers inhibit low-density lipoprotein oxidation by oxygen radicals. *Cardiovasc. Drugs Ther.* **10**:417–424 (1996).
12. D. Mauzerall and F. H. Westheimer. 1-Benzylidihydronicotinamide-A-Model for Reduced DPN. *J. Am. Chem. Soc.* **77**:2261–2264 (1955).
13. R. J. Abeles, R. F. Hutton, and F. H. Westheimer. The reduction of thioketones by model for a coenzyme. *J. Am. Chem. Soc.* **79**:712–716 (1957).
14. W. J. Baedel and R. J. Haas. Electrochemical oxidation of NADH analogs. *Anal. Chem.* **42**:918–927 (1970).
15. R. S. Varma and D. Kumar. Manganese triacetate mediated oxidation of Hantzsch 1,4-dihydropyridines to pyridines. *Tetrahedron Lett.* **40**:21–24 (1999).
16. Y.-Z. Mao, M.-Z. Jin, Z.-L. Liu, and L.-M. Wu. Oxidative reactivity of S-nitrosoglutathione with Hantzsch 1,4-dihydropyridine. *Org. Lett.* **2**:741–742 (2000).
17. X.-Q. Zhu, B.-J. Zhao, and J.-P. Cheng. Mechanism of the oxidations of NAD(P)H model Hantzsch 1,4-dihydropyridines by nitric oxide and its donor N-methyl-N-nitrosotoluene-p-sulfonamide. *J. Org. Chem.* **65**:8158–8163 (2000).
18. S. Moncada, R. M. J. Dalmer, and E. A. Higgs. Nitric oxide: physiology, pathophysiology and pharmacology. *Pharmacol. Rev.* **43**:109–142 (1991).
19. M. Kirsch and H. Groot. Reaction of peroxyxynitrite with reduced nicotinamide nucleotides, the formation of hydrogen peroxide. *J. Biol. Chem.* **274**:24664–24670 (1999).
20. J. Berson and E. Brown. Studies on dihydropyridines. I. The preparation of unsymmetrical 4-aryl-1,4-dihydropyridines by the Hantzsch-Beyer synthesis. *J. Am. Chem. Soc.* **77**:444–447 (1955).
21. D. M. Stout and A. I. Meyers. Recent advances in the chemistry of dihydropyridines. *Chem. Rev.* **82**:223–243 (1982).
22. V. Misik, A. Stasko, D. Gergel, and K. Ondrias. Spin-trapping and antioxidant properties of illuminated and non-illuminated nifedipine and nimodipine in heart homogenate and model system. *Mol. Pharmacol.* **40**:435–439 (1994).
23. J. Ogle, J. Stradins, and L. Baumann. Formation and decay of free cation radicals in the course of electrooxidation of 1,2- and 1,4-dihydropyridines (Hantzsch esters). *Electrochim. Acta* **39**:73–79 (1994).
24. J. Ludvik and F. Turecek, and J. Volke. Electrochemical oxidation mechanism of 4-disubstituted 1,4-dihydropyridines in acetonitrile. *J. Electroanal. Chem.* **189**:105–109 (1985).
25. R. A. More O'Ferrall. In: *Proton Transfer Reactions*. V. Gold and E. F. Caldin (eds.), Substrate Isotope Effects. Chapman and Hall, London, 1975, pp. 201–261.
26. J. Klima, J. Ludvik, J. Volke, M. Krikava, and V. Skala, and J. Kuthan. Spin trapping in electrochemical processes: trapping of radical intermediates in the electro-oxidation of substituted 1,4-dihydropyridines. *J. Electroanal. Chem.* **161**:205–211 (1984).
27. N. Ramamurthy, Srividya, P. Shanmugasundaram, and V. T. Ramakrishnan. Synthesis, characterization, and electrochemistry of some acridine-1,8-dione dyes. *J. Org. Chem.* **61**:5083–5089 (1996).
28. L. J. Núñez-Vergara, J. C. Sturm, A. Alvarez-Lueje, C. Olea-Azar, C. Sunkel, and J. A. Squella. Electrochemical oxidation of 4-methyl-1,4-dihydropyridines in protic and half aprotic. *J. Electrochem. Soc.* **146**:1478–1485 (1999).
29. J. Ludvik, J. Klima, J. Volke, and A. Kurfurst, and J. Kuthan. Electrochemical oxidation of substituted 1,4-dihydropyridines in non-aqueous acetonitrile. *J. Electroanal. Chem.* **138**:131–138 (1982).
30. J. Kuthan, M. Ferles, J. Volke, and N. Koshmina. The significance of a cyclic π -septet in some reactions of pyridine and its salts. *Tetrahedron* **26**:4361–4366 (1970).
31. R. H. Bocker and P. Guengerich. Oxidation of 4-alkyl-substituted 2,6-dimethyl-3,5-bis(alkoxycarbonyl)-1,4-dihydropyridines by human liver microsomes and immunochemical evidence for the involvement of a form of cytochrome P-450. *J. Med. Chem.* **29**:1596–1603 (1986).